

# Optimizing Nickel Doping in $\text{La}_{0.7}\text{Sr}_{0.3}\text{Ti}_{0.15}\text{Fe}_{0.85-x}\text{Ni}_x\text{O}_{3-\delta}$ Perovskite as a Potential Cathode Material for LT-SOFC

Ahmadani Darul Fikri<sup>1</sup>, Markus Diantoro<sup>1,2</sup>, Hartatiek<sup>1</sup>, Della Puspita Rahmadhani<sup>1</sup>, Ishmah Luthfiyah<sup>3</sup>, and Nasikhudin<sup>1,1</sup>

<sup>1</sup>Department of Physics, Faculty of Mathematics and Natural Science, Universitas Negeri Malang, Jl. Semarang 5, Malang 65145, Indonesia.

<sup>2</sup>Center of Advanced Materials for Renewable Energy, Universitas Negeri Malang, Jl. Semarang 5, Malang 65145, Indonesia.

<sup>3</sup>Integrated Science and Innovation, Institute of Science, Suranaree University of Technology, Nakhon Ratchasima, Thailand

**Abstract.** Solid Oxide Fuel Cells (SOFCs) are among the most efficient and environmentally friendly technologies. The cathode is a crucial component of SOFC system, a high-performance cathode material must exhibit high conductivity, good catalytic activity and structural stability toward the oxygen reduction reaction (ORR). In this study, the sol-gel method was used to prepare  $\text{La}_{0.7}\text{Sr}_{0.3}\text{Ti}_{0.15}\text{Fe}_{0.85-x}\text{Ni}_x\text{O}_{3-\delta}$  ( $x=0, 0.1, 0.2, 0.3$ ) powders and investigated for its potential as a cathode material for LT-SOFC. The phase, crystal structure, microstructure, morphology, and conductivity were characterized with varying Ni compositions. X-ray diffraction characterization reveals orthorhombic perovskite structure with space group *Pnma*. With increasing Ni content, the unit cell volume initially expanded but slightly contracted at  $x = 0.3$ , attributed to the smaller ionic radius of  $\text{Ni}^{3+}$  compared to  $\text{Fe}^{2+}$ . The LSTFN powders exhibit an interconnected network-like morphology consisting of fine particles and pores. All samples showed good homogeneity, uniform particle distribution, and high porosity. Electrical conductivity increased with Ni doping, reaching a maximum value of  $8.97 \text{ S}\cdot\text{m}^{-1}$  at room temperature for  $x = 0.2$ , more than twice that of the undoped sample. Further Ni content at  $x = 0.3$ , conductivity decreased may due to unit cell contraction. Therefore, the Ni composition of  $x = 0.2$  is identified as the optimal concentration for enhancing performance. These results suggest that LSTFN is a potential cathode material for LT-SOFC.

## 1 Introduction

Global energy demands continue to increase, while fossil fuel resources are becoming scarce. In addition, the use of fossil fuels has major impact on the environment due to release of greenhouse gases. This contributes to global warming and accelerates extreme climate change [1]. Therefore,

---

<sup>1</sup> Corresponding author: [nasikhudin.fmipa@um.ac.id](mailto:nasikhudin.fmipa@um.ac.id)

the solution regarding sustainable and environmentally friendly are needed to reduce the use of fossil fuels [2].

Hydrogen is the most potential renewable energy resources for energy production and storage due to its abundance in nature and its environmentally friendly characteristics, as it doesn't produce carbon emission. In addition, hydrogen has a high energy density and is relatively easy to store and transport [3]. One of the technologies that can utilize hydrogen as a fuel is Solid Oxide Fuel Cell (SOFC). SOFC is an energy conversion technology that operates through the electrochemical reaction between a fuel ( $H_2$ ) and an oxidant ( $O_2$ ) using a solid ion-conducting ceramic electrolyte [4].

In recent years, SOFCs have attracted considerable attention because of their high energy efficiency and conversion rates. Moreover, SOFCs offer greater fuel flexibility compared to other types of fuel cell, as they can operate using hydrogen, hydrocarbon, and biogas [5]. However, several challenges remain, particularly the requirement for high operating temperatures, which lead to high system cost, electrode degradation, and poor long-term stability. Therefore, reducing the operating temperature is currently a major challenge in SOFC development.

In SOFC, cathode has a crucial role in electrochemical performance. Cathode material must be able to support the oxygen reduction reaction (ORR) effectively. Good cathode material must have high electrical conductivity, good catalytic activity, and match in TEC with electrolyte materials [6]. Mixed ionic and electronic conductivity (MIEC) perovskite materials are widely used cathode material at intermediate-low temperatures [7]. Among MIEC materials, Cobalt-based perovskites are commonly used and showed superior performance at intermediate-low temperatures [8]. However, Cobalt-based perovskite materials have limitations including low chemical stability, high cost, and mismatch in thermal TEC with electrolyte materials [9].

$La_{0.7}Sr_{0.3}Ti_{0.15}Fe_{0.85}O_{3-\delta}$  (LSTF) is a cobalt-free material that has potential as a cathode material for low-intermediated temperature SOFCs. LSTF is a combination of  $La_{1-x}Sr_xTiO_{3-\delta}$  (LST) and  $La_{1-x}Sr_xFeO_{3-\delta}$  (LSF), which has high conductivity, good electrocatalytic, and higher chemical stability than cobalt-based materials [10]. LSTF has been widely studied as a cathode material for SOFCs due to its MIEC properties and promising electrochemical performance. However, its electrical conductivity and oxygen reduction reaction (ORR) activity of LSTF remain insufficient at low-intermediate operating temperature ( $<700^\circ C$ ), leading to reduced cathode performance. B-site substitution with transition-metal elements is an effective strategy to enhance charge transport and ORR kinetics. Nickel, which exhibits high electronic conductivity and has been successfully used to improve the electrochemical performance of  $La_{1-x}Sr_xMnO_3$  [11]. Nevertheless, a systematic study on nickel substitution in the LSTF system is still limited.

In this study, nickel was substituted into  $La_{0.7}Sr_{0.3}Ti_{0.15}Fe_{0.85-x}Ni_xO_{3-\delta}$  (LSTFN) with  $x = 0, 0.1, 0.2, \text{ and } 0.3$ . The obtained materials were characterized using XRD, SEM, and four-point probe measurement for electrical conductivity. The results were further analyzed and discussed by comparison with previous studies.

## 2 Experimental

### 2.1 Powder Synthesis

The LSTFN powders were synthesized via the sol-gel technique, as shown in Fig. 1.  $La(NO_3)_3 \cdot 6H_2O$  ( $\geq 99.9\%$ , Merck Millipore),  $Sr(NO_3)_2$  ( $\geq 99\%$ , Merck Millipore),  $TiCl_4$  ( $99.9\%$ , Sigma-Aldrich),  $Fe(NO_3)_3 \cdot 9H_2O$  ( $\geq 99\%$ , Merck Millipore),  $Ni(NO_3)_2 \cdot 6H_2O$  ( $\geq 98\%$ , Merck Millipore) were used as raw materials. First, stoichiometric amounts of the raw materials corresponding to the nominal composition  $La_{0.7}Sr_{0.3}Ti_{0.15}Fe_{0.85-x}Ni_xO_{3-\delta}$  ( $x = 0, 0.1, 0.2, 0.3$ ) were dissolved in 100 mL of deionized water and stirred at  $80^\circ C$  for 4 hours using a hot plate stirrer until

a clear solution was obtained. The solution was further heated at 180°C to evaporate the water until dark brown gel was formed. Subsequently, the gel was drained at 150°C (12 h) and calcined at 1000°C for 10 hours with a heating rate of 5°C/min. Finally, the LSTFN powders were obtained.

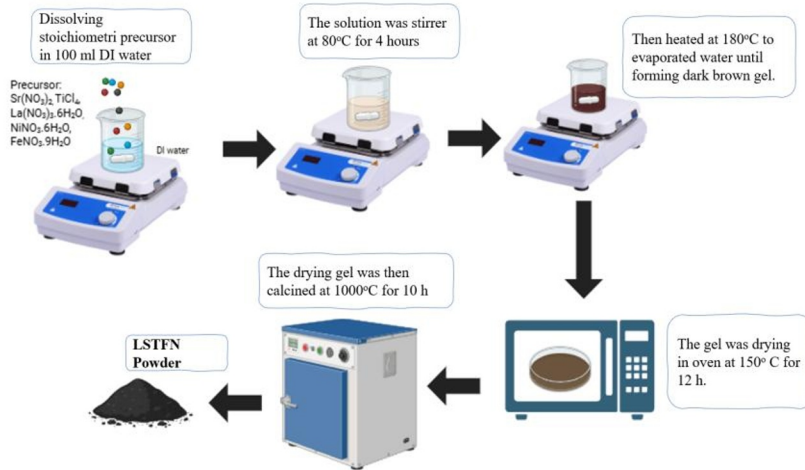


**Fig. 1.** LSTFN powder synthesis process via sol-gel method.

## 2.2 Materials Characterization

the phase and crystal structure of the LSTFN powders were characterized by XRD, the morphology was analyzed by SEM, and elemental composition was determined by EDX. The LSTFN powders were pressed into pellets with a diameter of 1 cm and a thickness of 3 mm, followed by sintering at 1000°C for 6 hours, as shown in Fig. 2. The LSTFN pellets were subsequently subjected to four-point probe (FPP) measurement to determine their electrical conductivity. The electrical conductivity measurement was repeated at least two times, and the average value was reported. Temperature-dependent electrical conductivity measurements were not performed due to limitations of the available measurement setup. therefore, the room-temperature conductivity was used as a comparative indicator to evaluate the influence of Ni substitution among different compositions.

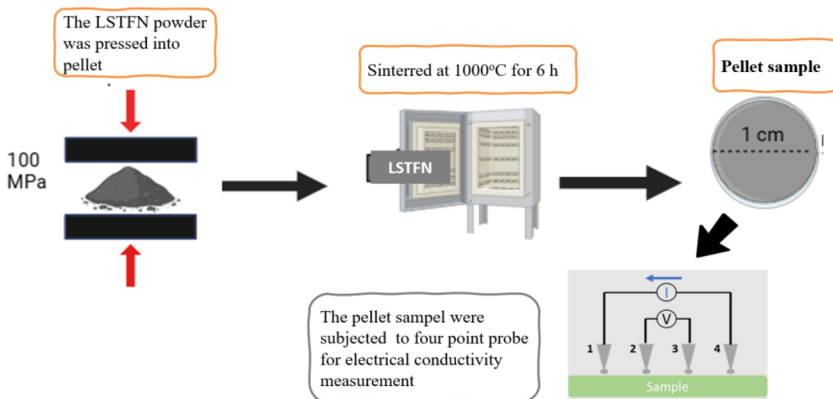


**Fig. 2.** Pelletization LSTFN sample probes for electrical conductivity measurement.

### 3 Results and Discussion

#### 3.1 Crystal Structure of LSTFN

The results of XRD characterization of the LSTFN powders calcined at 1000°C for 10 hours are illustrated on Fig. 3a. The XRD results indicate that all samples exhibit a perovskite-type structure with orthorhombic *Pnma* space group (Fig. 3c). Main diffraction peaks corresponding to the (101), (200), (220), (202), (231), (242), and (402). Percentages of phase purity around 81-76% and decrease with increasing Ni content, it indicating the presence of minor secondary phase in all samples. As we can see in Fig. 3a, small additional peaks with sign (#) are obtained, it corresponds to  $\text{LaSrFeO}_4$  phase. Crystallite size also decreases with increasing Ni content, showing that incorporation Ni ions into lattice inhibits the growth of grains during synthesis. And crystallinity values are nearly constant (37-40%), that meaning substitutes Ni ion to Fe ion is not significantly affect on overall structure.

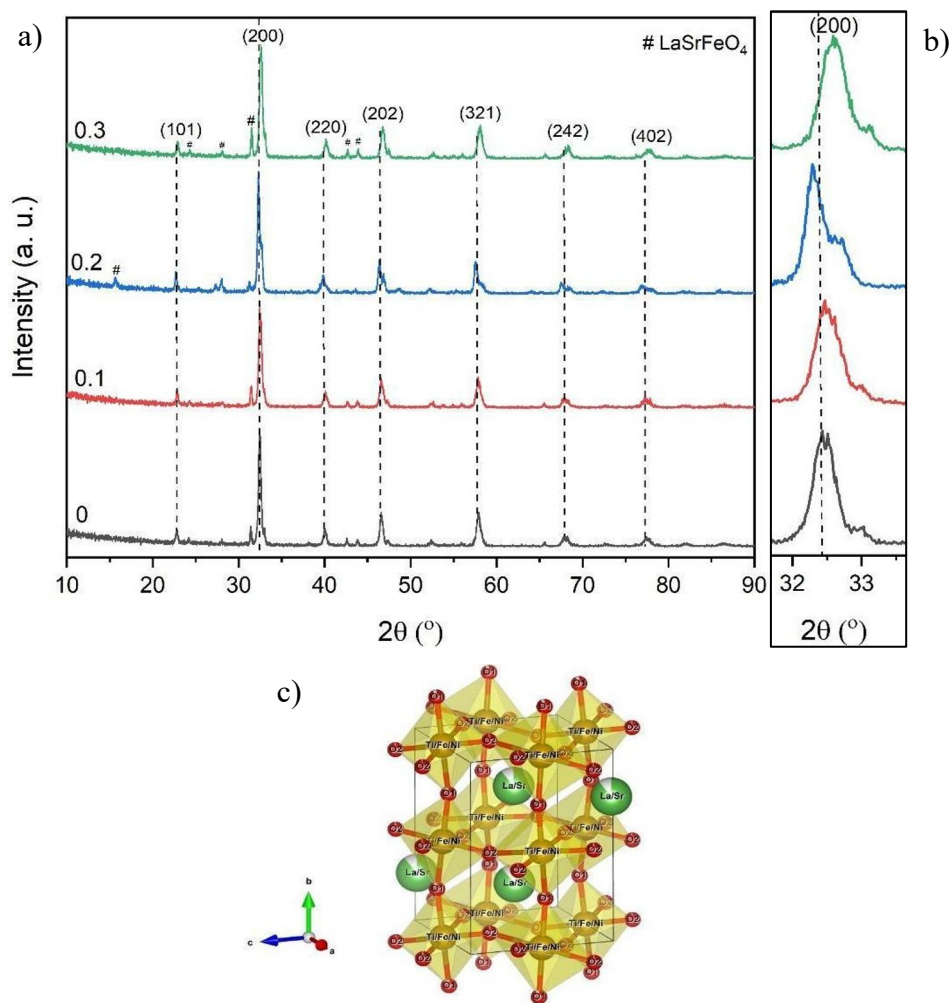


**Fig. 3.** a) XRD pattern of LSTFN, b) Magnified at  $2\theta$  from 32 to 33.5, c) LSTFN crystal structure visualization

**Table 1.** Phase purity, crystallite size, and crystallinity of LSTFN.

Ni Content (x)	Phase Purity (%)	Crystallite Size (nm)	Crystallinity (%)
0	81.2	20.8	38.3
0.1	79.6	18.9	37.2
0.2	78.5	17.5	38.0
0.3	76.3	18.7	39.9

**Table 2.** Lattice parameter of LSTFN at *Pnma* space group.

Ni Content (x)	Lattice Parameter (Å)			
	a	b	c	V
0	5.501(±0.002)	7.791(±0.003)	5.536(±0.001)	237.26(±0.03)
0.1	5.543(±0.001)	7.840(±0.001)	5.495(±0.001)	238.76(±0.03)
0.2	5.551(±0.001)	7.852(±0.002)	5.478(±0.001)	238.80(±0.12)
0.3	5.501(±0.001)	7.786(±0.001)	5.553(±0.001)	237.82(±0.03)

**Table 3.** Atom position of all samples LSTFN at *Pnma* space group.

Ni Content (x)	Atom Position											
	La/Sr			Ti/Fe/Ni			O <sub>1</sub>			O <sub>2</sub>		
	x	y	z	x	y	z	x	y	z	x	y	z
0	0.01	0.25	-0.003	0.00	0.00	0.50	0.49	0.25	0.08	0.26	0.02	-0.29
0.1	0.02	0.25	-0.005	0.00	0.00	0.50	0.48	0.25	0.03	0.21	0.04	-0.25
0.2	0.02	0.25	-0.002	0.00	0.00	0.50	0.51	0.25	0.00	0.29	0.05	-0.23
0.3	0.01	0.25	-0.003	0.00	0.00	0.50	0.48	0.25	0.06	0.30	0.02	-0.23

XRD pattern of the main peaks around 32,4 $\theta$  were magnified in Fig. 3b. A slightly shifts of the main with increasing Ni content can be observed, suggesting that Ni ions have been successfully incorporated into the perovskite lattice. To further analyze the effect of Ni incorporation, the lattice parameters of LSTFN were calculated and summarized in table 2. The lattice parameter increases with increasing Ni content, indicating lattice expansions, which generally occurs when dopant ions with larger ionic radii substitute smaller ions. This lattice expansion is consistent with the substitution of Fe<sup>3+</sup> (0.64 Å) by Ni<sup>2+</sup> (0.74 Å), which has a larger ionic radius. With further increasing Ni content to x = 0,3, the diffraction peaks shift toward higher angles, indicating a contraction of the unit cell. Considering the relative ionic radii, this behavior may suggest that Ni<sup>2+</sup> preferentially substitutes Fe<sup>2+</sup>, since Ni<sup>2+</sup> have as smaller ion radius than Fe<sup>2+</sup>(0.76 Å). Similar lattice contraction behavior has been reported in Ni-doped SFM perovskite by Dai [12], which was attributed to the preferential substitution of Fe<sup>2+</sup>/Fe<sup>3+</sup> ions by Ni<sup>2+</sup> ions to their comparable ionic radii. Tabel 3 shown the atomic position of A-sites

(La/Sr), B-sites (Ti/Fe/Ni), and Oxygen (O1 and O2) atoms, its remain in orthorhombic (Pnma) sites. Only small shifts positions are observed suggest a slight lattice distortion caused by Ni and Fe have distinct ionic radii. It indicating that Ni ions successfully substitute for Fe sites without changing the overall structure.

### 3.2 Morphology of LSTFN

Fig. 4 shows SEM images of the LSTFN cathode powder after calcination at 1000°C for 10 hours. The SEM images shows that all samples exhibit a connected network-like microstructure composed by pores and particle. The highly porous microstructure facilitates gas diffusion, electron and oxygen ion transport, also provides more active site for oxygens reduction reaction (ORR) in SOFC cathode application. The particle sizes were calculated and summarized in table 5. The average particle size increases at higher Ni content. Fig. 4 reveals that the particles are slightly agglomerated, however, the particles are well distributed and connected.

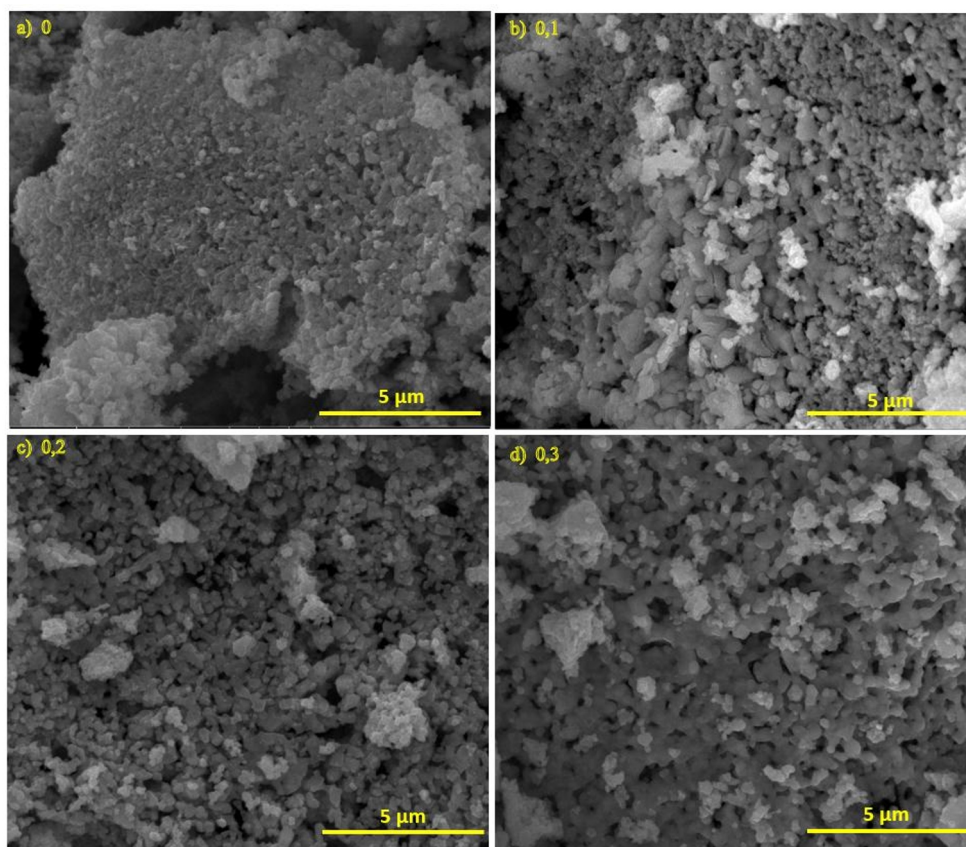
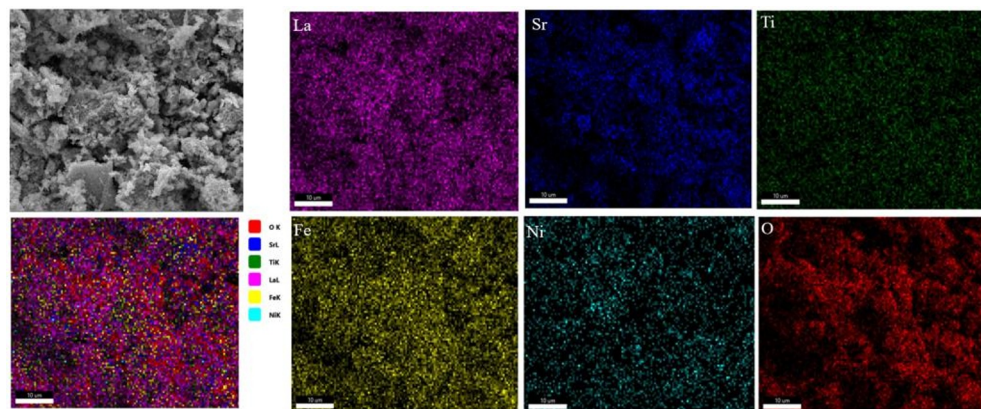


Fig. 4. SEM image of all LSTFN samples.

Table 5. Particle size of LSTFN.

Ni Content (x)	Particle Size (nm)
0	112 ( $\pm 3.7$ )
0.1	148 ( $\pm 7.1$ )
0.2	152 ( $\pm 5.9$ )
0.3	258 ( $\pm 11$ )

Fig. 5 demonstrates the EDX mapping results of LSTFN. The result confirm that all elements are uniformly distributed, indicating the materials have good chemical homogeneity, and that the Ni elements is successfully incorporated into the samples. Table 4 summarizes the atomic percentage of each element obtained from EDX analysis. It can be seen that the Ni atomic percentage increases with the doping level. These values are in agreement with synthesized composition. In addition, slight fluctuations in the La and Sr contents were observed. this irregularity indicates that part of La and Sr element may separate from the main perovskite phase to form a secondary phase, which was also confirmed in by the XRD results.



**Fig. 5.** EDX mapping result of LSTFN.

**Table 5.** Atomic element percentage of  $\text{La}_{0.7}\text{Sr}_{0.3}\text{Ti}_{0.15}\text{Fe}_{0.85-x}\text{Ni}_x\text{O}_{3-6}$ .

Element	Atomic (%)			
	x = 0	x = 0.1	x = 0.2	x = 0.3
La	13.94	15.86	12.62	15.82
Sr	11.51	5.98	14.28	4.20
Ti	1.91	1.27	1.11	2.67
Fe	11.19	14.51	7.41	9.27
Ni	0.00	2.27	4.95	5.94
O	61.46	60.12	59.64	62.09

### 3.3 Conductivity of LSTFN

Mixed ionic and electronic conductivity (MIEC) perovskite cathode materials such as LSTFN exhibit both electric and ionic charge transport, which are essential for oxygen reduction reaction (ORR) activity in SOFC systems. The major contribution in air is due to electric transport, while the ionic contribution is relatively lower. In this study, the electrical conductivity of LSTFN was measured using a four-point probe in air at room temperature, and the result are summarized in table 6. The relationship between Ni content and electrical conductivity are shown in Fig. 6. The conductivity increases with Ni doped samples. Highest conductivity was found in Ni x = 0,2. its reach until  $9 \times 10^{-4} \text{ S}\cdot\text{m}^{-1}$  at room temperature, more than twice higher then undoped sample. This result is higher than those reported in previous study on conventional perovskite material such as  $\text{La}_{0.7}\text{Sr}_{0.3}\text{MnO}_{3-6}$  ( $2.2 \times 10^{-4} \text{ S}\cdot\text{m}^{-1}$  at room temperature) [13], and Co-based perovskite such as  $\text{La}_{0.2}\text{Sr}_{0.8}\text{CoO}_{3-6}$  ( $4.5 \times 10^{-11} \text{ S}\cdot\text{m}^{-1}$ ) [14]. although the absolute conductivity values measurement at room temperature are lower than those typically required for practical SOFC cathode operation,

the observed enhancement with Ni substitution indicates improved electronic charge transport, which is beneficial for oxygen reduction reaction (ORR) kinetic in MIEC cathodes. Further increasing Ni at  $x = 0.3$  results in decrease in electrical conductivity, it may be associated with the increased presence of the secondary phases at  $x = 0.3$ , as observed in the XRD analysis.

**Table 6.** Electrical conductivity of LSTFN at room temperature.

Ni Content (x)	Conductivity ( $\text{Sm}^{-1}$ ) $\times 10^{-4}$
0	3.84
0.1	7.69
0.2	8.97
0.3	4.10

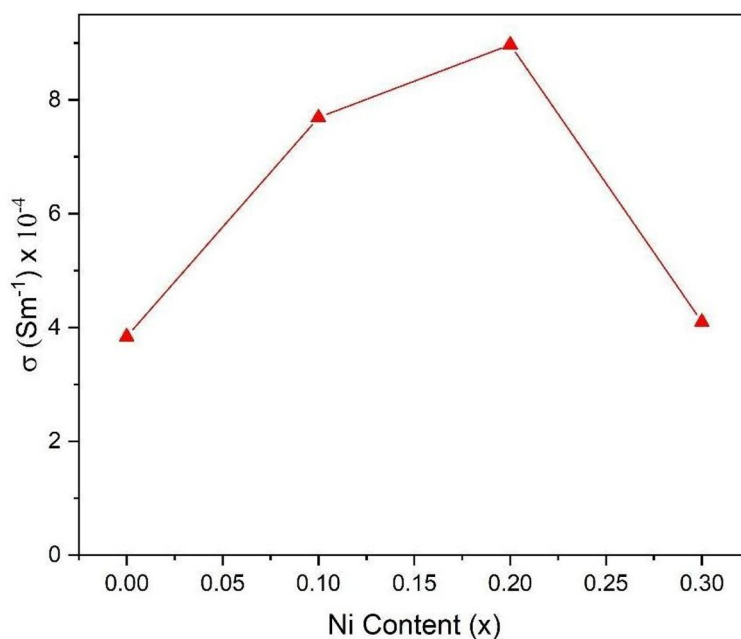


**Fig. 6.** Graph of Ni content depend on conductivity of LSTFN at room temperature.

Based on Fig. 6, that electrical conductivity increases with increasing Ni doping level, but decreases at  $x = 0.3$ . In addition, unit cell volume of LSTFN exhibits a similar trend, as shown in Fig. 7a. Based on the Table 2, the unit cell volume initially expands with Ni substitution, however, at  $x = 0.3$  volume slightly shrinks, which may be associated with changes in the  $\text{Fe}^{2+}/\text{Fe}^{3+}$  ratio induced by Ni incorporation. This similar trend suggests a qualitative correlation between unit cell and electrical conductivity. In Fe-based perovskite, electronic conduction is often described by a small polaron hopping mechanism, in which charge carriers hop between adjacent  $\text{Fe}^{2+}/\text{Fe}^{3+}$  sites and are highly sensitive to local structure distortion and valence variation [15]. To further examine this correlation, the bond distances and bond angles were analyzed, as these structural parameters can influence electronic transport by modifying the hopping pathways

of localized charge carriers. The average interatomic bond distances and angles show trends similar to those of the unit cell volume and electrical conductivity (Fig. 7b–d).

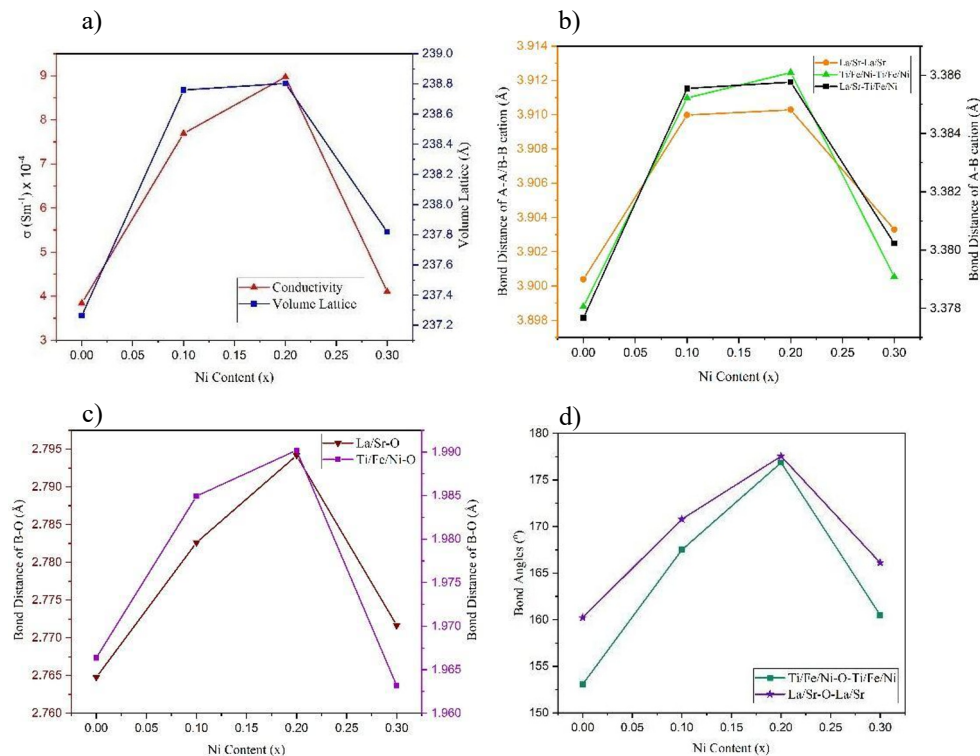


**Fig. 7.** a) Correlation of conductivity and lattice parameter, b) bond distances of inter-cation, c) bond distance of A/B Atoms-Oxygen, d) bond angles of A/B-Oxygen-A/B atom.

Based on Fig. 7a, sample with a larger unit cell exhibit higher electrical conductivity. This behavior may be associated with increased bond distances in the Fe/Ni-O-Fe/Ni network, which weakens the bonding strength and facilitates charge carrier hopping between neighboring. On the other hand, the decrease in electrical conductivity at  $x = 0.3$  may be related to the higher bonding strength associated with a smaller unit cell, where the reduced interatomic distance can enhance electron localization and restrict polaron hopping. A similar behavior has been reported for Ni-doped SFM-based perovskite by Dai et al [12]. In addition, the bond angles of A-O-A and B-O-B cations also influences on electrical conductivity. Bond angles approaching  $180^\circ$  provides a more linier conduction pathway, which is favorable for small polaron hopping with reduced structural distortion. Fig. 7d shows A-O-A and B-O-B bond angles of LSTFN. With increasing Ni content, the bond angles closer to  $180^\circ$ , followed by a slight decrease at  $x = 0.3$ . This trend qualitatively correlates with the observed electrical conductivity values. The improved electrical conductivity is expected to enhance electron transport to the active reaction sites, thereby facilitating the oxygen reduction reaction (ORR) and lowering the charge transfer resistance in SOFC cathodes.

It should be noted that temperature dependent electrical conductivity measurements were not conducted in this study due to limitations of the available experimental setup. Therefore, the discussion presented here is limited to room-temperature conductivity, which is used as a comparative parameter to evaluate the influence of Ni substitution on the structural and electrical properties of LSTFN.

## 4 Conclusion

LSTFN materials were successfully synthesized by the sol-gel method and their microstructure, structural, and electrical conductivity were systematically investigated. SEM analysis of LSTFN revealed a highly porous interconnected microstructure that is favorable for gas diffusion, which is beneficial for cathode applications. Average particles size are increased at high Ni content. The EDX mapping confirmed that the all samples have good homogeneity. XRD characterization confirmed the dominant orthorhombic perovskite (*Pnma*) phase in all samples, with slight decrease in phase purity at higher Ni content. Ni substitution modified the lattice parameters and the Fe/Ni-O-Fe/Ni conduction network, which expanded with increasing Ni content and further contracted at  $x = 0.3$  due to the smaller ionic radius of  $\text{Ni}^{2+}$  replacing  $\text{Fe}^{+2}$ . These structural changes influence the small polaron hopping mechanism and consequently the electrical conductivity. The sample with  $x = 0.2$  exhibited the highest electrical conductivity ( $8.97 \text{ S}\cdot\text{m}^{-1}$  at room temperature), more than twice that of undoped sample, indicating an optimal Ni content for charge transport. Then enhanced electrical conductivity is expected to facilitate electron transport to reaction sites and support oxygen reduction reaction (ORR) kinetics in SOFC cathodes. Although the conductivity was measured only at room temperature, the observed trends suggest that LSTFN is a promising MIEC cathode material for LT-IT SOFCs.

## References

1. M Diantoro, I. Istiqomah, O. Puji Dwi Lestari, et al, *Mater. Sci. Energy Tech.* **6**:368–381 (2023).
2. M. Diantoro, N.I. Muthi Aturroifah, I. Luthfiah, et al, *Carbon Resources Convers.* **8** (2025).
3. A. Pareek, R. Dom, J. Gupta, et al, *Mater. Sci. Energy Tech.* **3**,319–327 (2020).
4. M. Ilbas, B. Kumuk, J. of the Energy Inst. **92**, 682–692 (2019).
5. M. Singh, D. Zappa, E. Comini, *Int J Hydrogen Energy* **46**, 27643–27674 (2021).
6. M. Bilal Hanif M, M. Motola, S. qayyum, *et al*, *Chem. Eng. J.* 428 (2022).
7. N. N. M. Tahir, N. A. Baharuddin, A. A. Samat, *et al*, *J Alloys Compd.* 894 (2022).
8. P. V. Subhashini, K. V. D. Rajesh, *Mater. Today. Proc.* **62**, 2357–2361 (2022).
9. D. Shang, B. Zhang, L. Zhang, *et al*, *Chem. Eng. J.* 506 (2025).
10. M. Z. Ahmad, S. H. Ahmad, R. S. Chen, *et al*, *Emerg. Mater.* **8**, 3627–3637 (2025).
11. S. Manishanma, A. Dutta, *Mater. Chem. Phys.* 297 (2023).
12. N. Dai, J. Feng, Z. Wang, *et al*, *J. Mater. Chem. A Mater.* **1**, 14147–14153 (2013).
13. G. Jayakumar, D. Poomagal, P. Akshadha, *et. al*, *J. of Mater. Sci.: Mater. In Elec.* **23**, 20945–20953 (2020).
14. N. Alhokbany, S. Almotairi, J. Ahmed, S. Al-Saeedi, T. Ahamad, S. Al-Shehri, *J. of King Saud Univ. – Sci.* **4** (2021).
15. T. L. Rao, S. Dash, *Appl Phys A Mater Sci Process* 131(2025).